

Structural parameters and oxygen ion conductivity of $\text{Y}_2\text{O}_3\text{--ZrO}_2$ and MgO--ZrO_2 at high temperature

Sanghyeon Yoon^a, Taimin Noh^a, Wook Kim^b, Joo Choi^b, Heesoo Lee^{a,*}

^a*School of Materials Science & Engineering, Pusan National University, Busan 609-735, Republic of Korea*

^b*Steelmaking Research Group, Technical Research Laboratories, POSCO, Pohang 790-785, Republic of Korea*

Received 31 March 2013; received in revised form 8 May 2013; accepted 8 May 2013

Available online 16 May 2013

Abstract

The oxygen ion conductivity of zirconia-based solid electrolytes doped with 8 mol% $\text{Y}_2\text{O}_3\text{--ZrO}_2$ (YSZ) and 9 mol% MgO--ZrO_2 (Mg-PSZ) at high temperature was investigated in terms of their thermal behavior and structural changes. At room temperature, YSZ showed a single phase with a fluorite cubic structure, whereas Mg-PSZ had a mixture of cubic, tetragonal and some monoclinic phases. YSZ exhibited higher ionic conductivity than Mg-PSZ at temperatures from 600 °C to 1250 °C because of the existence of the single cubic structure and low activation energy. A considerable increase in the conductivity with increasing temperature was observed in Mg-PSZ, which showed higher ionic conductivity than YSZ within the higher temperature range of 1300–1500 °C. A monoclinic-to-tetragonal phase transformation was found in Mg-PSZ and the lattice parameter of the cubic phase increased at 1200 °C. The phase transformation and the large lattice free volume contributed to the significant enhancement of the ionic conductivity of Mg-PSZ at high temperatures.

© 2013 Elsevier Ltd and Techna Group S.r.l. All rights reserved.

Keywords: B. X-ray methods; C. Ionic conductivity; D. ZrO_2 ; Structural change

1. Introduction

Zirconia-based solid electrolytes have attracted considerable interest because of their excellent mechanical strength, transport properties and thermal stability in both oxidizing and reducing atmospheres [1,2]. These materials are used as an electrolyte for solid oxide fuel cells (SOFC), oxygen sensor and pump for deoxidizing of molten steel [3,4]. When divalent or trivalent cations (e.g., Ca^{2+} , Mg^{2+} and Y^{3+}) are substituted for tetravalent Zr^{4+} ions, oxygen vacancies O^{2-} are introduced for charge compensation [5]. The vacancies act as mobile electrical charge carriers because oxygen ions are transported by hopping along their vacancy sites.

The effects of dopant size, concentration and valence state on the ionic conductivity have been considered on the basis that the cation substitution in ZrO_2 is accompanied by changes in structure, vacancy concentration and defect association energy [6]. Since these changes can affect the oxygen ion

conductivity, it is important to prove the correlation between the conductivity and the dopant type in ZrO_2 [7].

Many studies have been performed to improve the ionic conductivity of the electrolytes, particularly the $\text{Y}_2\text{O}_3\text{--ZrO}_2$ system, owing to their superb ionic conductivity [8–9]. The MgO--ZrO_2 system, exhibiting better mechanical and thermal properties than the $\text{Y}_2\text{O}_3\text{--ZrO}_2$, is suitable for high temperature applications [10]. However, previous studies have generally been focused on 8 mol% YSZ at SOFCs operating temperatures (800–1000 °C). The research concerning ionic conductivity of the electrolytes for oxygen pump as a high temperature application is insufficient. In order to improve the performance of oxygen pump for removing oxygen in molten steel, the investigation of the conduction mechanism of $\text{Y}_2\text{O}_3\text{--ZrO}_2$ and MgO--ZrO_2 systems at high temperatures (around 1500 °C) is required.

This paper discusses the structural dependence of the oxygen ion conductivity of 8 mol% $\text{Y}_2\text{O}_3\text{--ZrO}_2$ and 9 mol% MgO--ZrO_2 . The ionic conductivity was examined at temperatures up to 1500 °C, and the thermal behavior and structural parameters of the electrolytes were analyzed to verify their conduction behaviors.

*Corresponding author. Tel.: +82 51 510 2388; fax: +82 51 512 0528.

E-mail address: heesoo@pusan.ac.kr (H. Lee).

2. Experimental procedure

Zirconia powders doped with 8 mol% Y_2O_3 (Tosoh corporation, TZ-8Y) and 9 mol% MgO (Saint-Gobain ZirPro, MgZ02B) were used as raw materials. The powders were formed into a rectangular (length 60 mm; width 7 mm) steel die under a uniaxial pressure of 20 MPa, and then sintered at 1600 °C for 6 h in ambient atmosphere.

X-ray diffraction (XRD, PANalytical, X'Pert-Pro) patterns of the sintered powder were collected at room temperature over a 2θ range of 20–90° with a scan speed of 1°/min and a scan step of 0.02°/2 θ . In situ high-temperature XRD was conducted to determine the structural changes at 1200 °C. The lattice parameter was refined by Rietveld analysis using the whole pattern refinement module of PANalytical X'Pert HighScore Plus software. The shape of the XRD peak and the background, were fitted to a pseudo-Voigt function and a fifth-degree polynomial, respectively. Scanning electron microscopy (SEM, Hitachi, S-4800) was performed to characterize the surface morphology and grain size of the electrolytes.

The ionic conductivity of the electrolytes was measured using a four-probe dc conductivity technique over the temperature range of 600–1500 °C. The specimens were cut into rectangular shapes ($2.5 \times 5.5 \times 40 \text{ mm}^3$). Four notches were formed to tightly wind up the Pt electrode wires, and Pt paste was applied to the wires and the notches to ensure connection between the electrolytes with the electrode. This was followed by calcination at 1000 °C for 1 h. Direct current was supplied by a current source (Keithley, 2400), and the corresponding voltage drop was collected using a multimeter (Agilent, 34401A). Differential scanning calorimetry (DSC, TA Instruments Ltd., Q200) was used to determine the phase transformation of the YSZ and Mg-PSZ sintered powders, and thermograms were obtained over a temperature range of 25–1500 °C at a heating rate of 5 K/min.

3. Results and discussion

Fig. 1 shows XRD patterns of the YSZ and Mg-PSZ powders after sintering at 1600 °C. YSZ occurred as a single phase with a fluorite cubic structure, whereas Mg-PSZ exhibited a mixture of cubic, tetragonal and monoclinic phases. The tetragonal and monoclinic phases were observed when the MgO content in ZrO_2 was below 12–13 mol%, which corresponds to the equilibrium phase for the ZrO_2 –MgO system [11]. The lattice parameter of the cubic phase was refined by Rietveld analysis of the XRD patterns, to determine the effects of the dopant cations (Y^{3+} and Mg^{2+}) on the structural parameters. A cubic structure with a lattice parameter of 5.137 Å was identified in YSZ due to the substitution of Y^{3+} ($r=1.019 \text{ Å}$ [12] in eight-fold coordination) for Zr^{4+} ($r=0.84 \text{ Å}$ [12]) sites. The lattice parameter of the cubic phase of Mg-PSZ was 5.0774 Å because the ionic radius of Mg^{2+} ($r=0.89 \text{ Å}$ [13]) was similar to that of Zr^{4+} .

SEM images in Fig. 2 show the surfaces of sintered YSZ and Mg-PSZ. Coarse grains, $>5 \mu\text{m}$ in size, and a small grain-boundary surface area were observed in YSZ, whereas

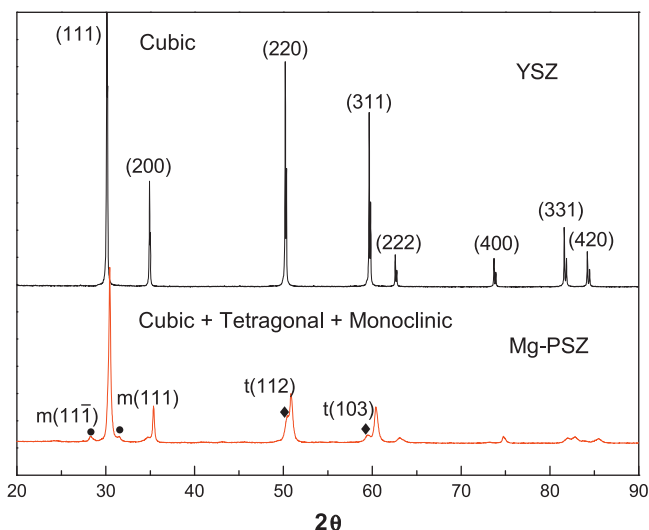


Fig. 1. XRD patterns of YSZ and Mg-PSZ powders after sintering at 1600 °C.

the microstructure of Mg-PSZ was mainly composed of coarse grains larger than 10 μm . Some small grains representing the monoclinic phase were formed at the grain boundaries in Mg-PSZ (indicated by arrows in Fig. 2b) [8]. This result corresponds to the XRD patterns as shown in Fig. 1. It is well known that the ionic conductivity of zirconia-based electrolytes depends on their crystal structure, because the cubic structure has higher ionic mobility than the tetragonal or the monoclinic structure [5]. Therefore, YSZ with a single cubic phase, is predicted to have high ionic conductivity.

Fig. 3 presents the oxygen ion conductivity of the YSZ and Mg-PSZ from 600 °C to 1000 °C. The conductivity was calculated using the following equation:

$$\sigma = (C/T) \exp(-E_a/kT) \quad (1)$$

where σ is the ionic conductivity, C is the pre-exponential factor, T is the absolute temperature, E_a is the activation energy and k is Boltzmann's constant ($8.6173324 \times 10^{-5} \text{ eV/K}$). At 600 °C, the ionic conductivity of YSZ was $7.33 \times 10^{-3} \text{ S cm}^{-1}$ and that of Mg-PSZ was $3.44 \times 10^{-4} \text{ S cm}^{-1}$. Their conductivities increased linearly with the increase in temperature up to 1000 °C, and YSZ exhibited higher conductivity than Mg-PSZ over the whole temperature range. However, Mg-PSZ showed a considerable increase in conductivity. The conductivities at 1000 °C were $6.83 \times 10^{-2} \text{ S cm}^{-1}$ and $2.15 \times 10^{-2} \text{ S cm}^{-1}$ for YSZ and Mg-PSZ, respectively.

In contrast, the electrolytes exhibited different conduction behaviors in the high temperature range of 1000–1500 °C, as illustrated in Fig. 4. Mg-PSZ showed higher ionic conductivity than YSZ at temperatures above 1300 °C. It is expected that the oxygen permeation property of the oxygen pump with Mg-PSZ will be excellent because of its high ionic conductivity within the high temperature range (1300–1500 °C). The slope of the Arrhenius plots of Mg-PSZ gradually increased with increasing temperature, whereas the slope of YSZ was almost constant. This suggests that the ionic conductivity of Mg-PSZ was significantly enhanced by increasing temperature. Takahashi and Iwahara reported a similar

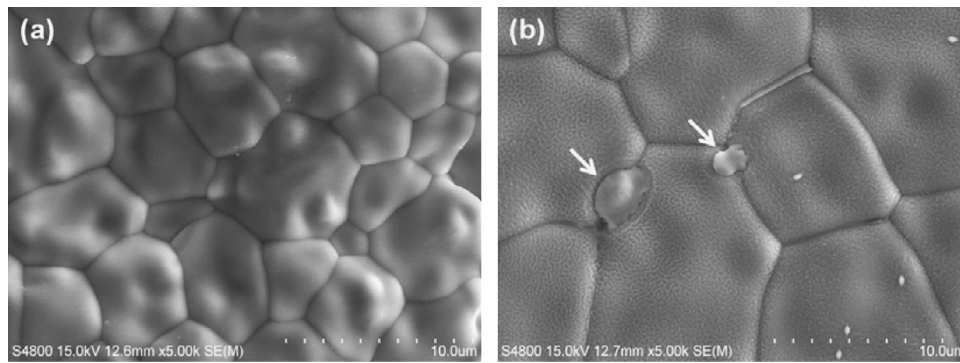


Fig. 2. SEM images of the surface of sintered (a) YSZ and (b) Mg-PSZ.

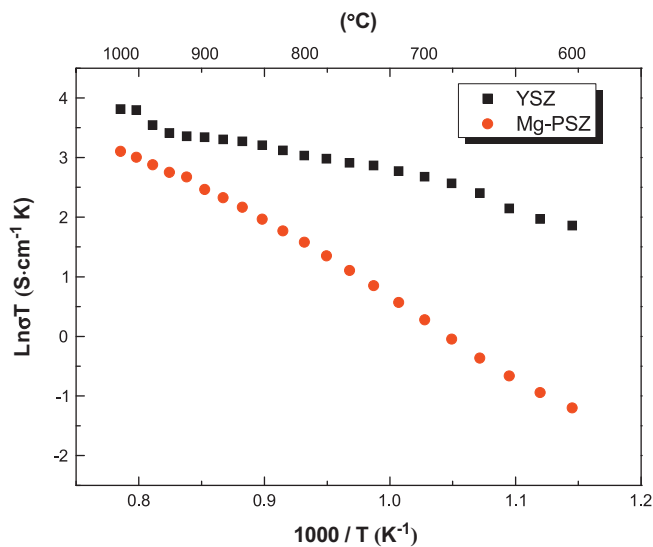


Fig. 3. Oxygen ion conductivity of YSZ and Mg-PSZ from 600 °C to 1000 °C.

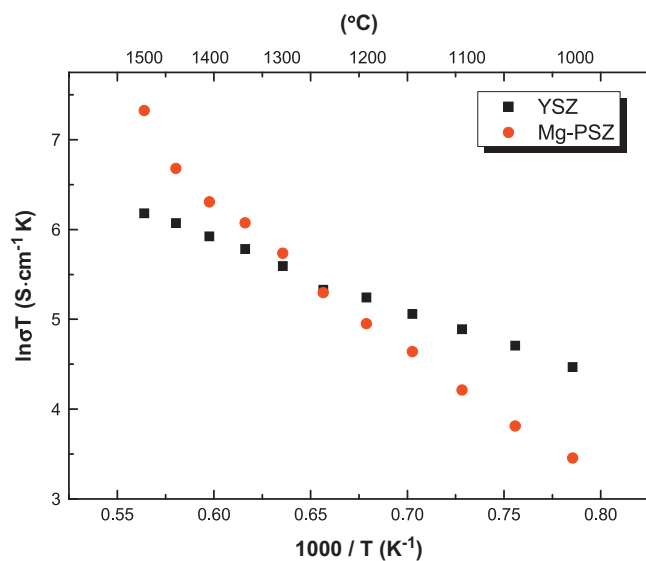


Fig. 4. Arrhenius plots of oxygen ion conductivity of YSZ and Mg-PSZ from 1000 °C to 1500 °C.

tendency for a rapid increase in ionic conductivity of pure Bi_2O_3 in a certain temperature range, which was confirmed by a phase transformation [14]. This conductivity reversion was attributed to the phase transformation, to the structural changes in Mg-PSZ, or perhaps both.

The activation energy of YSZ and Mg-PSZ were derived from the Arrhenius plots of the conductivity, and are listed in Table 1. The plots in the lower temperature range of 600–1000 °C were linear, with activation energies of 0.48 eV and 1.11 eV for YSZ and Mg-PSZ, respectively. The activation energy of Mg-PSZ increased considerably from 1.24 eV to 1.81 eV in the higher temperature range. The increase of activation energy at higher temperatures is caused by electronic conductivity. It is probable that the oxygen partial pressure decreases during conductivity measurement at high temperature, which leads to the increase of electronic conductivity and activation energy [15]. When large dopant cations are substituted for Zr^{4+} ions, the ionic conductivity is reduced by a steric blocking effect. The large cations can disturb the migration of oxygen vacancies more effectively, which can lead to an increase in activation energy [6]. Mg-PSZ had less of a mismatch in the ionic radii of the dopant and host cations. For this reason, it exhibited superior ionic conductivity compared to YSZ, within the high temperature range (1300–1500 °C), in spite of the higher activation energy. The discrepancies between the activation energy and the ionic conductivity can be explained by defect association and oxygen vacancy concentration.

Badwal reported that the vacancy concentration of M^{3+} doped ZrO_2 was approximately 3.75%, and that of M^{2+} doped ZrO_2 was 6–6.5% [8]. ZrO_2 with alkaline earth metal cations (M^{2+}) was less effective than rare earth cations (M^{3+}) because the M^{2+} cation substitution can lead to an increase in defect association (dopant–vacancy interaction), reducing the vacancy mobility [16]. Mg-PSZ exhibited poor conductivity below 1000 °C because of the high activation energy by defect association, and the existence of the tetragonal and the monoclinic phase. On the other hand, its superior conductivity compared to YSZ was inferred by the large oxygen vacancy concentration and by the fact that there was sufficient energy to overcome the defect association within the high temperature range (1300–1500 °C).

Table 1
Activation energy (E_a) and ionic conductivity values of YSZ and Mg-PSZ.

Electrolytes	E_a (eV) Low temp.	E_a (eV) High temp.		Conductivity σ (S cm ⁻¹)	
	600–1000 °C	1000–1250 °C	1250–1500 °C	At 1000 °C	At 1500 °C
YSZ	0.48	0.58	0.70	6.83×10^{-2}	2.72×10^{-1}
Mg-PSZ	1.11	1.24	1.81	2.15×10^{-2}	8.54×10^{-1}

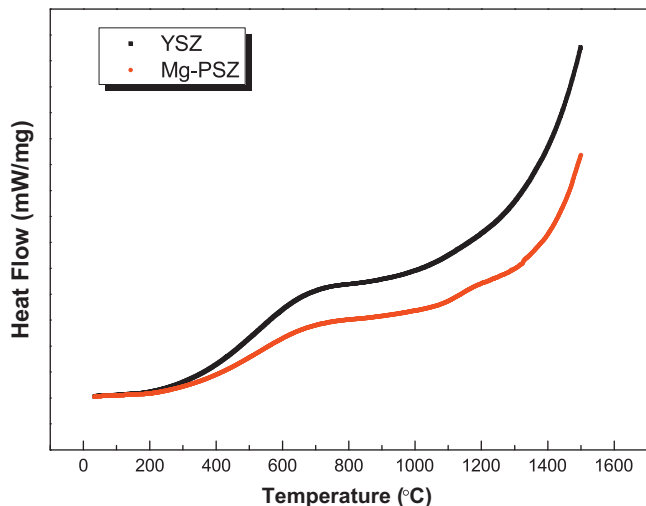


Fig. 5. DSC thermogram curves of YSZ and Mg-PSZ as a function of temperature.

The thermal behavior was examined by DSC to determine whether structural changes in YSZ and Mg-PSZ occurred at high temperature. In Fig. 5, both YSZ and Mg-PSZ exhibited a dominant peak around 700 °C. This peak is associated with the formation of the oxygen vacancies by losing the lattice oxygen with increasing temperature [17]. A small exothermic peak (corresponding to the monoclinic-to-tetragonal phase transformation) was observed around 1200 °C in Mg-PSZ. The monoclinic phase with large lattice distortion, leads to a high degree of anisotropy of oxygen sites thus disturbing oxygen ion hopping [18]. Generally, partially-stabilized zirconia exhibits two or three phases according to the dopant concentration, and the monoclinic-to-tetragonal transformation occurred at approximately 1100–1200 °C. A small amount of the residual monoclinic phase transformed to the tetragonal phase at this temperature, and the transformation contributed to the increase in ionic conductivity.

Table 2 lists the parameters selected for the crystal structure of the electrolytes obtained from the Rietveld refinement of the HT-XRD patterns. The lattice parameters of the cubic phase for YSZ and Mg-PSZ increased to 5.202 Å and 5.146 Å at 1200 °C, respectively. The degree of increase in lattice the parameter was similar (0.065 Å and 0.069 Å), but Mg-PSZ had a large lattice free volume at high temperature due to the smaller ionic radius of Mg²⁺ (0.89 Å) compared with Y³⁺

Table 2
Structural parameters of YSZ and Mg-PSZ refined at room temperature and 1200 °C.

Electrolytes	Room temp.		High temp. (1200 °C)	
	a [Å]	V [Å ³]	a [Å]	V [Å ³]
YSZ	5.137	135.6	5.202	140.8
Mg-PSZ	5.077	130.9	5.146	136.3

(1.019 Å). Cook and Sammells reported that a larger lattice free volume provided more space for easy oxygen ion hopping [19]. The enhancement of ionic conductivity with increasing temperature was attributed to the increased lattice free volume which enabled the oxygen ions to move more easily.

4. Conclusions

The oxygen ion conductivity of 8 mol% Y₂O₃–ZrO₂ (YSZ) and 9 mol% MgO–ZrO₂ (Mg-PSZ) from 600 to 1500 °C was investigated. Mg-PSZ showed higher ionic conductivity than YSZ within the higher temperature range (1300–1500 °C). The ionic conductivities of YSZ and Mg-PSZ increased with increasing temperature, and were 2.72×10^{-1} S cm⁻¹ and 8.54×10^{-1} S cm⁻¹ at 1500 °C, respectively. Mg-PSZ exhibited the monoclinic-to-tetragonal phase transformation around 1200 °C, and this temperature led to an increase in the lattice parameter of the cubic phase. Mg-PSZ had a large lattice free volume because the ionic radius of Mg²⁺ (0.89 Å) is smaller than that of Y³⁺ (1.019 Å). The significant enhancement of ionic conductivity of Mg-PSZ was attributed to the phase transformation, and to the large lattice free volume providing more space for the easy movement of oxygen ions. Further investigation will be progressed to determine the conduction mechanism of the electrolytes by electrical and structural analyses.

Acknowledgment

This research was supported by POSCO.

References

- [1] S.R. Choi, N.P. Bansal, Mechanical behavior of zirconia/alumina composites, *Ceramics International* 31 (2005) 39–46.

- [2] W. Huang, P. Shuk, M. Greenblatt, M. Groft, F. Chen, M. Liu, Structural and electrical characterization of a novel mixed conductor: $\text{CeO}_2\text{--Sm}_2\text{O}_3\text{--ZrO}_2$ solid solution, *Journal of the Electrochemical Society* 147 (2000) 4196–4202.
- [3] K.C. Radford, R.J. Bratton, Zirconia electrolyte cells, *Journal of Materials Science* 14 (1979) 59–65.
- [4] H.W. Koo, H.J. Park, G.M. Choi, H.G. Lee, Electrochemical deoxidation of molten steel with application of an oxygen permeable membrane, *ISIJ International* 47 (2007) 689–698.
- [5] P. Aldebert, J.-P. Traverse, Structure and ionic mobility of zirconia at high temperature, *Journal of the American Ceramic Society* 68 (1985) 34–40.
- [6] J.A. Kilner, R.J. Brook, A study of oxygen ion conductivity in doped non-stoichiometric oxides, *Solid State Ionics* 6 (1982) 237–252.
- [7] V. Butler, C.R.A. Catlow, B.E.F. Fender, J.H. Harding, Dopant ion radius and ionic conductivity in cerium dioxide, *Solid State Ionics* 8 (1983) 109–113.
- [8] S.P.S. Badwal, Zirconia-based solid electrolytes: microstructure, stability and ionic conductivity, *Solid State Ionics* 52 (1992) 23–32.
- [9] X.J. Chen, K.A. Khor, S.H. Chan, L.G. Yu, Influence of microstructure on the ionic conductivity of yttria-stabilized zirconia electrolyte, *Materials Science and Engineering A* 335 (2002) 246–252.
- [10] W.-C.J. Wei, Y.-P. Lin, Mechanical and thermal shock properties of size graded MgO-PSZ refractory, *Journal of the European Ceramic Society* 20 (2000) 1159–1167.
- [11] C.T. Grain, Phase relations in the $\text{ZrO}_2\text{--MgO}$ system, *Journal of the American Ceramic Society* 50 (1967) 288–290.
- [12] R.D. Shannon, C.T. Prewitt, Effective ionic radii in oxides and fluorides, *Acta Crystallographica B* 25 (1969) 925–946.
- [13] M. Yashima, T. Hirose, M. Kakihana, Y. Suzuki, M. Yoshimura, Size and charge effects of dopant m on the unit-cell parameters of monoclinic zirconia solid solutions $\text{Zr}_{0.98}\text{M}_{0.02}\text{O}_{2-\delta}$ ($\text{M}=\text{Ce, La, Nd, Sm, Y, Er, Yb, SC, Mg, and Ca}$), *Journal of the American Ceramic Society* 80 (1997) 171–175.
- [14] T. Takahashi, H. Iwahara, High oxide ion conduction in sintered oxides of the system $\text{Bi}_2\text{O}_3\text{--WO}_3$, *Journal of Applied Electrochemistry* 3 (1973) 65–72.
- [15] H.J. Park, G.M. Choi, The electrical conductivity and oxygen permeation of ceria with alumina addition at high temperature, *Solid State Ionics* 178 (2008) 1746–1755.
- [16] V.V. Kharton, F.M.B. Marques, A. Atkinson, Transport properties of solid oxide electrolyte ceramics: a brief review, *Solid State Ionics* 174 (2004) 135–149.
- [17] R.K. Gupta, E.Y. Kim, Y.H. Kim, C.M. Whang, Effect of strontium ion doping on structural, thermal, morphological and electrical properties of a co-doped lanthanum manganite system, *Journal of Alloys and Compounds* 490 (2010) 56–61.
- [18] J. Richter, P. Holtappels, T. Graule, T. Nakamura, L.J. Gauckler, Materials design for perovskite SOFC cathodes, *Monatshefte für Chemie* 140 (2009) 985–999.
- [19] R.L. Cook, A.F. Sammells, On the systematic selection of perovskite solid electrolytes for intermediate temperature fuel cells, *Solid State Ionics* 45 (1991) 311–321.